

## **SUPPORTING INFORMATION**

### **METHODS**

#### **DSC screening studies for selection of HRN and mannitol ratio in NSD**

Physical mixtures of HRN and mannitol (HRN-M-PM) were prepared in 1:9, 2:8, 3:7, 4:6, 5:5, 6:4, 7:3, 8:2 and 9:1 proportion. The samples were heated in DSC pan upto 245 °C at a heating rate of 20 °C/min and quenched to 25 °C at 20 °C/min. The samples were then scanned in DSC at a rate of 20 °C/min upto 300 °C. Onset values of thermal events are reported in the results.

#### **Preparation of NSD batches**

NSDs of HRN-mannitol system were prepared using laboratory scale spray dryer (U228 Model, Labultima Ltd., Mumbai, India). Mixture of HRN and mannitol in 5:5 weight proportion was dissolved in methanol and water (7:3), to achieve a final composition of 2.0% (w/v) in the solvent mixture. The solution was spray dried at an inlet temperature of 60, 70, 80 and 90 °C, outlet temperature of 60 °C, feed rate of 3 mL/min, air atomization pressure of 0.95 kg/cm<sup>2</sup> and vacuum of 100 mm of water column. NSD of HRN-mannitol system was labeled as HRN-M, while, HRN-mannitol physical mixture was labeled as HRN-M-PM.

#### **Dissolution studies**

Dissolution analysis of HRN-M-PM and HRN-M was carried out in pH 6.8 phosphate buffer (50 mM) containing 0.125% sodium carboxy methyl cellulose (Na CMC) with a volume of 900 ml. USP/NF paddle method was used at a rotational speed of 100 rpm. Media was equilibrated to 37.0 ± 0.5 °C before the dissolution. HRN-M-PM and HRN-M equivalent to 30 mg HRN were added to dissolution apparatus (Electrolab USP-24, India). Samples were collected at 0, 5, 10, 20, 30, 40, 60, 120, 180 and 240 min. Samples were filtered through 0.1 µm filter stacked in the filtration assembly. Samples were analyzed by UV spectrophotometer at 288 nm. Dissolution profiles were constructed by plotting the cumulative percent drug released against time. Data was evaluated by application of student's t-test for assessing statistical significance of differences.

#### **Caco-2 and MCF-7 cell uptake study**

The cellular uptake of HRN was studied using C6-HRN-M and C6-HRN-M-PM. Details of methods are provided in the manuscript. The fluorescence images were acquired using CLSM.

## RESULTS

### DSC screening study for selection of HRN and mannitol ratio in NSD

Heat-cool-heat DSC scan of HRN generated its amorphous phase, which showed only a glass transition ( $T_g$ ) event at 72.7 °C and no recrystallization ( $T_c$ ) or melting ( $T_m$ ) was evident for this sample (Figure 2 of manuscript).

First heating runs of all samples showed melting of  $\beta$ -D mannitol at about 164 °C followed by melting of HRN at about 214 °C (data not shown).

In the cooling run, HRN converted into amorphous phase for HRN: mannitol proportion of 9:1, 8:2, 7:3, 6:4 and 5:5. HRN recrystallized in the cooling run itself for HRN: mannitol proportion of 4:6, 3:7, 2:8 and 1:9. For all proportions, mannitol recrystallized in the cooling run (data not shown).

Figure S1 shows second heating runs of HRN-M-PM samples. HRN showed  $T_g$  and  $T_c$  event for HRN: mannitol proportion of 9:1, 8:2, 7:3, 6:4 and 5:5 in the second heating run. Melting of HRN was not observed for these samples. HRN showed only melting (no  $T_g$  and  $T_c$  event) for HRN: mannitol proportion of 4:6, 3:7 and 2:8. For HRN: mannitol proportion of 1:9, no  $T_g$ ,  $T_c$  or  $T_m$  event was observed for HRN, which could be due to its very low proportion. For all proportions, mannitol showed only melting event(s). Table S1 summarizes thermal events for HRN and mannitol observed in the second heating run.

Mannitol caused plasticization of amorphous HRN by lowering its  $T_g$  (Table S1). Mannitol also altered recrystallization behavior of HRN. The plasticization and altered recrystallization behavior of HRN in presence of mannitol was attributed to crystallization inducing effect of mannitol. As 60% mannitol induced complete crystallization in HRN during cooling run itself, 50% mannitol was found to be the best minimum concentration for induction of crystallization in HRN. Lower concentrations of mannitol could have led to generation of partially amorphous phase of HRN, while higher concentrations of mannitol would have reduced the drug concentration, thereby increasing the excipient load and overall size of orally administered formulation. In order to keep the balance between complete crystallization of HRN and maximum possible drug loading, 5:5 was found to be the best proportion for generation of HRN-M NSD.

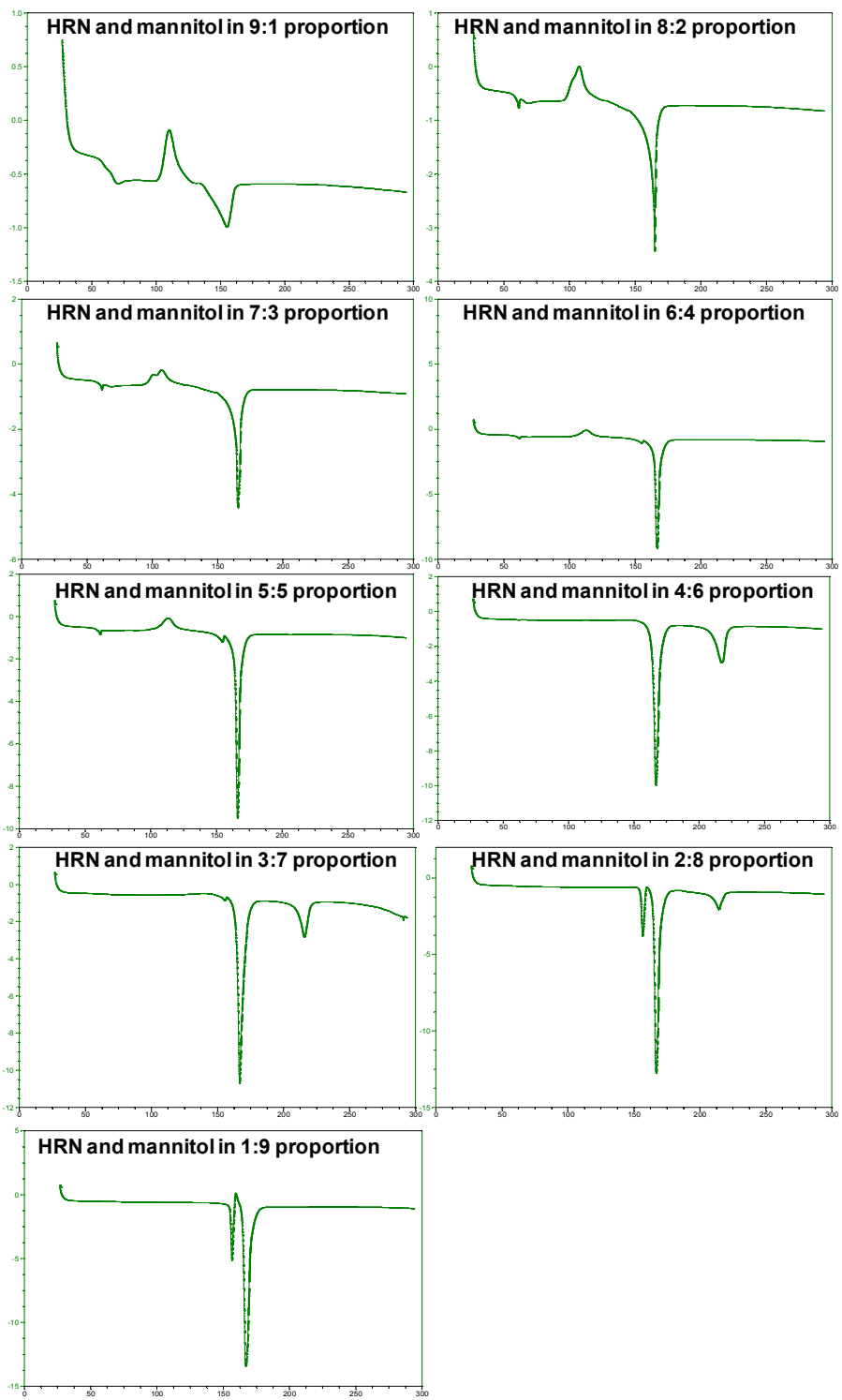


**Figure S1.** DSC scans of HRN-M-PM samples. Only second heating runs are shown.

**Table S1.** Thermal events of HRN and mannitol in the second heating run

HRN : mannitol ratio	HRN thermal events (°C)			Mannitol thermal events (°C)	
	$T_g$	$T_c$	$T_m$	$T_m$ ( $\delta$ polymorph)	$T_m$ ( $\beta$ polymorph)
9:1	64.2	103.8	-	154.9	-
8:2	59.6	96.9	-	-	163.2
7:3	59.4	95.2	-	-	163.7
6:4	59.2	104.2	-	151.2	164.6
5:5	59.2	103.4	-	153.0	164.2
4:6	-	-	209.4	-	164.1
3:7	-	-	210.9	-	164.3
2:8	-	-	208.5	154.8	164.7
1:9	-	-	-	154.9	164.6

**Evaluation of NSD batches**

The Scherrer equation, as mentioned in the paper, was used to estimate average crystallite size of HRN in HRN-M which is given as follows-

$$\tau = \frac{K\lambda}{B_t \cos\theta} \quad \text{Equation 3}$$

where,  $\tau$  is crystallite dimension, K is shape factor (0.9),  $\lambda$  is the wavelength and  $\beta_t$  is line broadening due to the effect of small crystallites, as measured by the full width of the PXRD peak at half-height. Specific diffraction peaks of HRN at  $2\theta$  values of  $7.19^\circ$ ,  $14.41^\circ$ ,  $16.94^\circ$ ,  $17.65^\circ$  and  $20.89^\circ$  were used for crystallite size analysis. Peak width at half maxima (PWHM) values for these peaks was determined. Table S2 shows crystallite size of HRN in various HRN-M batches obtained at different inlet temperatures.

Inlet temperature of  $60^\circ\text{C}$  resulted in generation of partially amorphous HRN while completely crystalline phase was obtained above  $70^\circ\text{C}$ . The crystallite size increased with increase in inlet temperature. Thus,  $70^\circ\text{C}$  inlet temperature value provided smallest possible size of crystallites with complete crystallinity and hence, this temperature was selected for generation of HRN-M, which was used for further studies.

**Table S2.** Crystallite size of HRN particles in HRN-M batches

Inlet temperature	Crystallite size of HRN
*60 °C	99.1 nm
70 °C	137.3 nm
80 °C	144.2 nm
90 °C	197.2 nm

\*Partially amorphous HRN phase was observed in this batch

### Dissolution analysis

Figure S2 shows dissolution profiles of HRN-M and HRN-M-PM in 50 mM pH 6.8 phosphate buffer containing 0.125% Na CMC with a volume of 900 ml. Dissolution of HRN-M was found to be higher than HRN-M-PM. NSD showed significant improvement in the rate and extent of dissolution. The difference in the dissolution profiles was found to be statistically significant by employing student's t test ( $p < 0.05$ ).

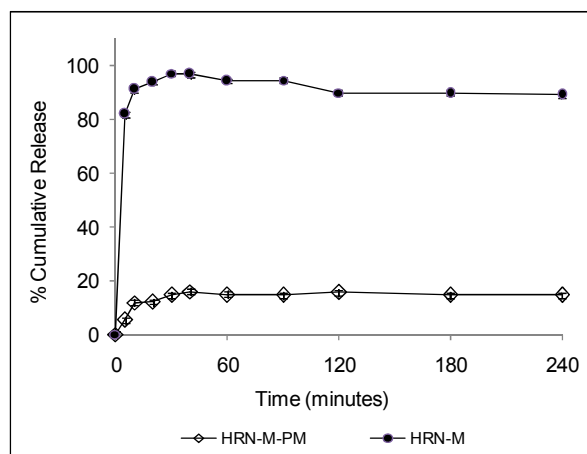


**Figure S2.** Dissolution profiles of HRN-M and HRN-M-PM PM in 50 mM pH 6.8 phosphate buffer containing 0.125% Na CMC with a volume of 900 ml

### Caco-2 and MCF-7 cell uptake study

The fluorescence in cell uptake study was observed due to coumarin 6 (C6) which dissolved along with HRN. Figure S3 shows CLSM images for cell uptake of C6, C6-HRN-M-PM and HRN-M in Caco-2 and MCF-7 cells. C6 did not penetrate in the cells effectively and exhibited poor fluorescence in the cells. The fluorescence of C6 was almost similar to that of C6-HRN-M-

PM, which indicated poor solubility behavior of microcrystalline HRN. However, with HRN nanocrystals, the penetration of C6 was found to be significantly higher which was attributed to higher apparent solubility and dissolution rate of HRN nanocrystals.

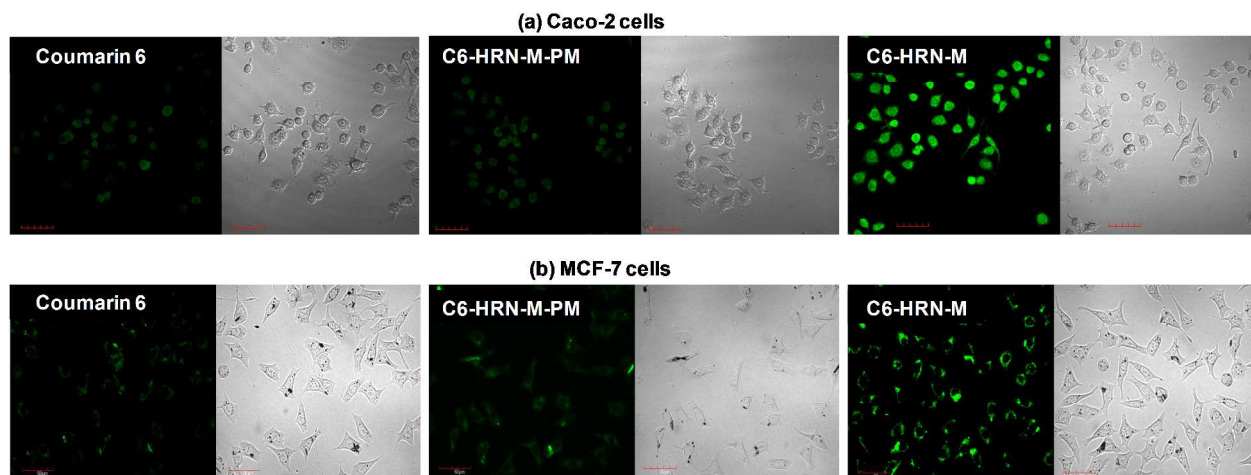


**Figure S3.** CLSM images of uptake study in (a) Caco-2 cells and (b) MCF-7 cells